Cell Reports

Non-canonical Caspase-1 Signaling Drives RIP2-Dependent and TNF-α-Mediated Inflammation *In Vivo*

Graphical Abstract

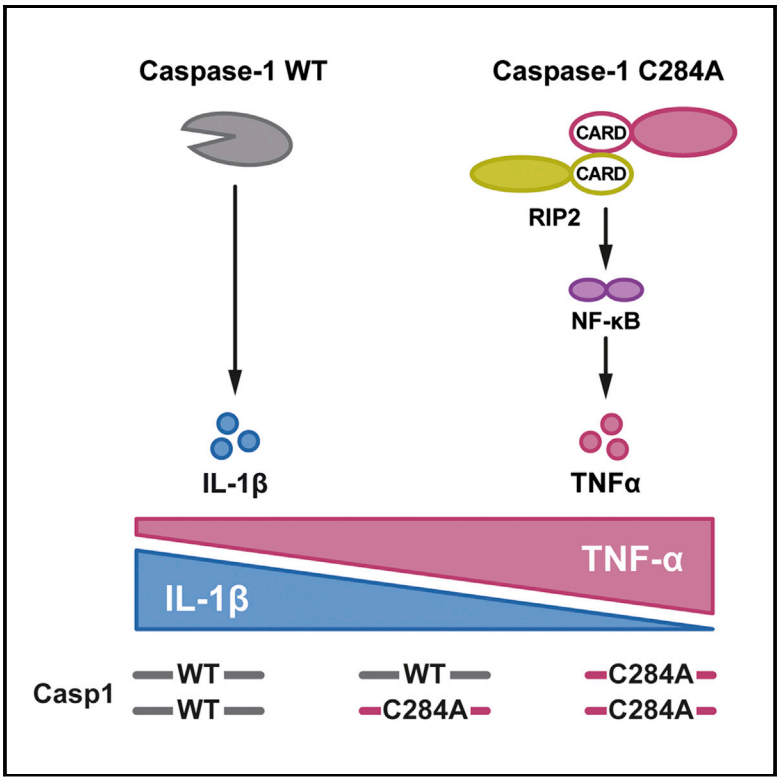

Authors

Sören Reinke, Mary Linge, Hans H. Diebner, ..., Joachim Roesler, Angela Rösen-Wolff, Stefan Winkler

Correspondence

stefan.winkler@uniklinikum-dresden.de

In Brief

Reinke et al. show that enzymatically inactive caspase-1-C284A mediates non-canonical caspase-1 signaling. This pathway is RIP2 dependent and mediated by TNF-α but independent from IL-1 cytokines.

Highlights

- Enzymatically inactive caspase-1-C284A induces pro-inflammatory signaling *in vivo*
- Caspase-1-C284A-mediated inflammation requires RIP2-dependent TNF-α secretion
- Caspase-1-C284A signaling is independent from NLRP3 inflammasome and IL-1 cytokines

Reinke et al., 2020, Cell Reports *30*, 2501–2511
February 25, 2020
https://doi.org/10.1016/j.celrep.2020.01.090

CellPress

Cell Reports
Report

Non-canonical Caspase-1 Signaling Drives RIP2-Dependent and TNF-α-Mediated Inflammation *In Vivo*

Sören Reinke,[1] Mary Linge,[1] Hans H. Diebner,[2] Hella Luksch,[1] Silke Glage,[3] Anne Gocht,[1] Avril A.B. Robertson,[4,5] Matthew A. Cooper,[5] Sigrun R. Hofmann,[1] Ronald Naumann,[6] Mihail Sarov,[7] Rayk Behrendt,[8] Axel Roers,[8] Frank Pessler,[9,10] Joachim Roesler,[1] Angela Rösen-Wolff,[1] and Stefan Winkler[1,11,*]

[1]Department of Pediatrics, University Hospital Carl Gustav Carus, Technische Universität Dresden, Dresden, Germany
[2]Institute for Medical Informatics and Biometry, Faculty of Medicine Carl Gustav Carus, Technische Universität Dresden, Dresden, Germany
[3]Institute for Laboratory Animal Science, Hannover Medical School, Hannover, Germany
[4]School of Chemistry and Molecular Biosciences, University of Queensland, Brisbane, Australia
[5]Institute for Molecular Bioscience, University of Queensland, Brisbane, Australia
[6]Transgenic Core Facility, Max Planck Institute of Molecular Cell Biology and Genetics, Dresden, Germany
[7]Genome Engineering Facility, Max Planck Institute of Molecular Cell Biology and Genetics, Dresden, Germany
[8]Institute for Immunology, Faculty of Medicine Carl Gustav Carus, Technische Universität Dresden, Dresden, Germany
[9]Twincore, Centre for Experimental and Clinical Infection Research, Hannover, Germany
[10]Helmholtz Centre for Infection Research, Braunschweig, Germany
[11]Lead Contact
*Correspondence: stefan.winkler@uniklinikum-dresden.de
https://doi.org/10.1016/j.celrep.2020.01.090

SUMMARY

Pro-inflammatory caspase-1 is a key player in innate immunity. Caspase-1 processes interleukin (IL)-1β and IL-18 to their mature forms and triggers pyroptosis. These caspase-1 functions are linked to its enzymatic activity. However, loss-of-function missense mutations in *CASP1* do not prevent autoinflammation in patients, despite decreased IL-1β production. *In vitro* data suggest that enzymatically inactive caspase-1 drives inflammation via enhanced nuclear factor κB (NF-κB) activation, independent of IL-1β processing. Here, we report two mouse models of enzymatically inactive caspase-1-C284A, demonstrating the relevance of this pathway *in vivo*. In contrast to *Casp1*$^{-/-}$ mice, caspase-1-C284A mice show pronounced hypothermia and increased levels of the pro-inflammatory cytokines tumor necrosis factor alpha (TNF-α) and IL-6 when challenged with lipopolysaccharide (LPS). Caspase-1-C284A signaling is RIP2 dependent and mediated by TNF-α but independent of the NLRP3 inflammasome. LPS-stimulated whole blood from patients carrying loss-of-function missense mutations in *CASP1* secretes higher amounts of TNF-α. Taken together, these results reveal non-canonical caspase-1 signaling *in vivo*.

INTRODUCTION

Pathogens, stress, and damage signals induce activation of caspase-1, typically mediated by proximity-induced autoproteolysis in multimeric protein complexes called inflammasomes. Caspase-1 then processes pro-interleuken (IL)-1β and pro-IL-18 into their activated secretory forms and also mediates pyroptosis, a programmed pro-inflammatory cell death, thereby initiating a pro-inflammatory immune response (Winkler and Rösen-Wolff, 2015). Dysregulated caspase-1 signaling is involved in the pathogenesis of numerous diseases, from rare autoinflammatory syndromes to more common diseases such as rheumatoid arthritis and gout (Saavedra et al., 2015). Originally, caspase-1-mediated pro-inflammatory signaling was thought to depend solely on its enzymatic activity.

We previously reported that loss-of-function missense mutations in *CASP1* are associated with autoinflammatory symptoms in patients, despite decreased IL-1β production (Heymann et al., 2014; Luksch et al., 2013). *In vitro* data suggest that enzymatically inactive caspase-1 may drive inflammation via enhanced activation of nuclear factor κB (NF-κB), independent of its enzymatic activity (Heymann et al., 2014; Lamkanfi et al., 2004; Sarkar et al., 2006). This signaling pathway depends on protein-protein interactions of pro-caspase-1 with RIP2 via their CARD domains (Heymann et al., 2014). Downstream of NOD2, a transient CARD-CARD domain interaction of NOD2 with RIP2 initiates the formation of a helical oligomeric structure of RIP2 (RIPosome), which finally activates NF-κB and mitogen-activated protein kinase (MAPK) pathways (Gong et al., 2018; Pellegrini et al., 2018). As caspase-1 also carries the death receptor domain CARD to mediate protein-protein interactions, enzymatically inactive caspase-1 may function as an alternative to NOD2. Furthermore, non-enzymatic scaffold functions, leading to pro-inflammatory signaling, have been described for caspase-8 and MALT1 (Fritsch et al., 2019; Gewies et al., 2014; Kang et al., 2015).

Recently published data show that murine myeloid cells or intestinal epithelial organoids deficient in the enzymatic activity of

caspase-1 (*Casp1*$^{-/-}$ or *Casp1*$^{C284A/C284A}$) undergo an ASC- and caspase-8-dependent delayed form of cell death involving caspase-3 (Lee et al., 2018; Schneider et al., 2017; Van Opdenbosch et al., 2017). In the absence of caspase-1 enzymatic activity, cell death following activation of NLRP1b and NLRC4 inflammasomes had apoptotic features (Lee et al., 2018; Van Opdenbosch et al., 2017), while cell death following canonical stimulation of the NLRP3 inflammasome led to delayed lytic cell death accompanied by the release of mature IL-1β (Schneider et al., 2017). Toll-like receptor (TLR)-stimulated synthesis of the antiapoptotic protein c-FLIP was shown to inhibit caspase-8-induced apoptosis (Van Opdenbosch et al., 2017). Although comparison between *Casp1*$^{-/-}$ and *Casp1*$^{C284A/C284A}$ cells revealed no differences in terms of cell death or secretion of inflammatory cytokines in two of the studies, Van Opdenbosch et al. (2017) detected reduced activation of caspase-3/7 in *Casp1*$^{C284A/C284A}$ bone marrow-derived macrophages (BMDMs) following activation of the NLRC4 inflammasome compared with *Casp1*$^{-/-}$ BMDMs. Hypothetically, this could be caused by a caspase-1-C284A-mediated induction of c-FLIP via NF-κB.

In order to analyze the pro-inflammatory function of enzymatically inactive caspase-1 *in vivo*, we generated two genetic mouse models of enzymatically inactive caspase-1 p.C284A, using conditional gene targeting into the *Rosa26* locus as well as gene editing of the endogenous *Casp1* locus using CRISPR/Cas9. In contrast to *Casp1*$^{-/-}$ mice, both models of caspase-1-C284A show pronounced hypothermia and increased levels of the pro-inflammatory cytokines tumor necrosis factor alpha (TNF-α) and IL-6 when challenged with lipopolysaccharide (LPS) *in vivo*. Genetic and biochemical approaches revealed that caspase-1-C284A-mediated signaling is Rip2 dependent and mediated by TNF-α but independent of the NLRP3 inflammasome and IL-1 cytokines. LPS-stimulated whole blood from patients carrying loss-of-function missense mutations in *CASP1* secretes enhanced amounts of TNF-α, indicating the relevance of this pathway in humans. Taken together, these results demonstrate a non-canonical pathway of caspase-1-mediated signaling independent of its enzymatic activity *in vivo*.

RESULTS

R26-C284A Mice Do Not Suffer from Spontaneous Inflammation

To analyze enzymatically inactive caspase-1 *in vivo*, we generated a mouse model of caspase-1 p.C284A using conditional gene targeting into the *Rosa26* locus (Figures S1A–S1C). Subsequent deletion of the loxP site-flanked neomycin-stop-cassette using a PGK-Cre mouse line (Lallemand et al., 1998) and backcrossing to *Casp1*$^{-/-}$ background (Case et al., 2013) revealed the genotype *Rosa26*$^{Casp1\text{-}C284A/Casp1\text{-}C284A}$/*Caspase1*$^{-/-}$, hereafter referred to as R26-C284A (Figure S1D). These mice displayed robust and widespread expression of the pro-caspase-1 variant throughout various tissues (Figure S1E). R26-C284A mice are viable, develop normally, and show fertility and lifespan comparable with wild-type (WT) and *Casp-1*$^{-/-}$ mice (Figures S1F–S1I). As patients with loss-of-function missense mutations in *CASP1* are prone to develop symptoms of autoinflammation (Heymann et al., 2014), we screened R26-C284A mice for signs of spontaneous inflammation. R26-C284A mice displayed healthy fur without exanthema and no signs of arthritis, and immunophenotyping revealed a physiological distribution of essential myeloid and lymphoid cells (Figure S1J). Furthermore, histological analysis excluded infiltration of immune cells in spleen, liver, kidney, knee joint, lung, skin, small intestine, or colon, and spontaneous production of IL-1α, IL-1β, TNF-α, or IL-6 in serum of 11- or 66-week-old mice was ruled out (Figures S2A–S2C). These results indicate that murine inactive caspase-1 does not spontaneously induce inflammation. However, caspase-1/inflammasome signaling pathways are tightly regulated and experimental mice were kept under specific pathogen-free (SPF) conditions. As autoinflammatory diseases can be triggered by inflammatory stimuli, we further investigated R26-C284A mice following a sterile pro-inflammatory stimulus.

Enzymatically Inactive Caspase-1 Promotes Systemic Inflammation *In Vivo*

We challenged WT, *Casp1*$^{-/-}$, and R26-C284A mice with LPS (10 mg/kg intraperitoneal [i.p.]). In sub-thermoneutral ambient temperatures, mice respond to LPS with hypothermia, which can be used as surrogate for the severity of systemic inflammation (Rudaya et al., 2005). Following LPS stimulation, caspase-1-C284A mice showed pronounced hypothermia compared with *Casp1*$^{-/-}$ mice, thereby reflecting increased pro-inflammatory signaling mediated by expression of the enzymatically inactive caspase-1 *in vivo* (Figure 1A). However, the strongest hypothermia was seen in WT mice expressing the active protease.

The analysis of cytokines in the serum 24 h after LPS challenge revealed elevated levels of IL-1α and IL-1β in WT mice compared with *Casp1*$^{-/-}$ or R26-C284A mice (Figure 1B). Although activation of caspase-1 WT directly leads to activation and secretion of IL-1β, caspase-1-mediated induction of pyroptotic cell death may lead to passive efflux of IL-1α. Because inactive caspase-1 promotes activation of NF-κB *in vitro* (Heymann et al., 2014; Lamkanfi et al., 2004; Sarkar et al., 2006), we additionally assessed serum levels of the NF-κB targets IL-6 and TNF-α. R26-C284A mice expressed higher levels of IL-6 and TNF-α compared with *Casp1*$^{-/-}$ mice (Figure 1B), thereby indicating the *in vivo* relevance of the proposed mechanism of caspase-1-C284A-mediated activation of NF-κB. Of note, serum levels of IL-6 and TNF-α upon LPS stimulation were highest in WT mice.

To further characterize signaling pathways in R26-C284A mice, we performed a multiplex assay and analyzed the cytokine pattern in serum 24 h after application of the inflammatory stimulus. This assay confirmed the described patterns for the cytokines IL-1α, IL-1β, IL-6, and TNF-α (data not shown). Compared with *Casp1*$^{-/-}$ mice, R26-C284A mice expressed higher levels of the pro-inflammatory cytokines IL-2, IL-9, IL-22, IL-18, IL-27, and IFN-γ (Figure 1C). Interestingly, expression of IL-2, IL-9, IL-22, IL-27, and IFN-γ is known to be a direct or indirect target of NF-κB, thereby further supporting the hypothesis that expression of inactive caspase-1 mediates NF-κB activation *in vivo* (Hoyos et al., 1989; Liu et al., 2007; Serfling et al., 1989; Sica et al., 1997; Zhu et al., 1996).

Additionally, NF-κB activation was analyzed using a luciferase reporter assay. Overexpression of murine caspase-1 WT or

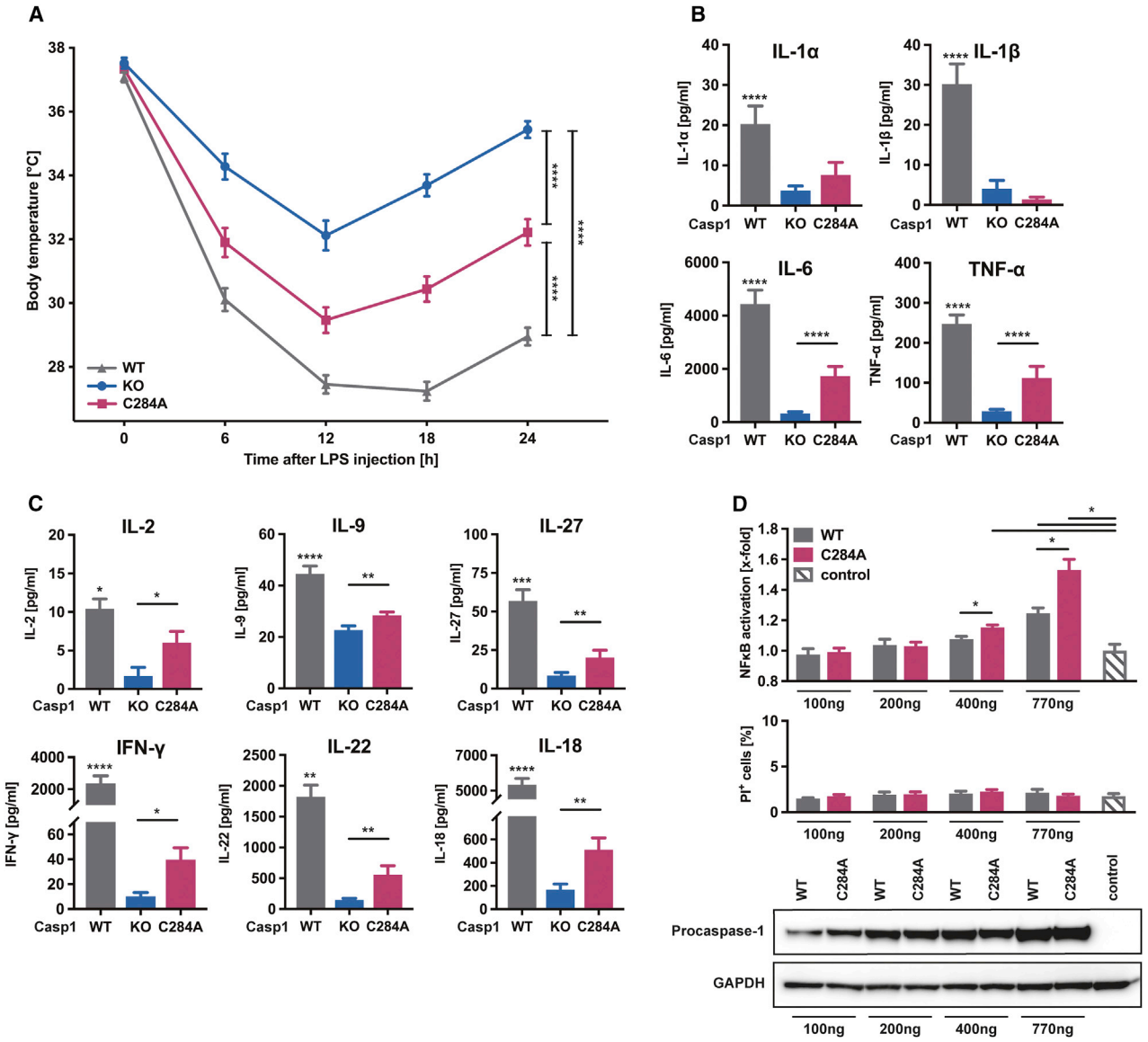

Figure 1. Expression of Enzymatically Inactive Caspase-1 Promotes Systemic Inflammation *In Vivo*

(A) Mice of the indicated genotypes were challenged with 10 mg/kg LPS i.p., and body temperature was measured every 6 h.

(B) Serum levels of indicated cytokines 24 h after LPS challenge.

(C) Multiplex cytokine analysis of serum 24 h after LPS challenge.

(D) HEK293T cells were transiently transfected with plasmids coding for murine Casp1 WT or C284A mutant. NF-κB activation was measured using a luciferase reporter gene assay, cell death was quantified using propidium iodide dye exclusion, and expression of caspase-1 was analyzed by western blotting.

In (A) and (B), data are presented as mean ± SEM, n = 22–30 per group. In (C), data are presented as mean ± SEM, n = 10 per group. In (D), data are presented as mean ± SEM, n = 4 per group.

C284A mutant in HEK293T cells led to a dose-dependent activation of NF-κB compared with control (Figure 1D). In reaction to increasing protein expression, caspase-1-C284A enhanced activation of NF-κB compared with caspase-1 WT. Differential NF-κB activation was induced neither by varying protein expression between caspase-1 WT and C284A mutant nor by altered cell death rates (Figure 1D).

Caspase-1-C284A-Initiated Inflammation Is RIP2 Dependent and TNF-α Mediated

We and others have previously demonstrated that enzymatically inactive caspase-1 interacts with RIP2, thereby mediating NF-κB activation *in vitro* (Heymann et al., 2014; Lamkanfi et al., 2004; Sarkar et al., 2006). In order to analyze the RIP2 dependency of caspase-1-C284A-mediated signaling *in vivo*, we crossed

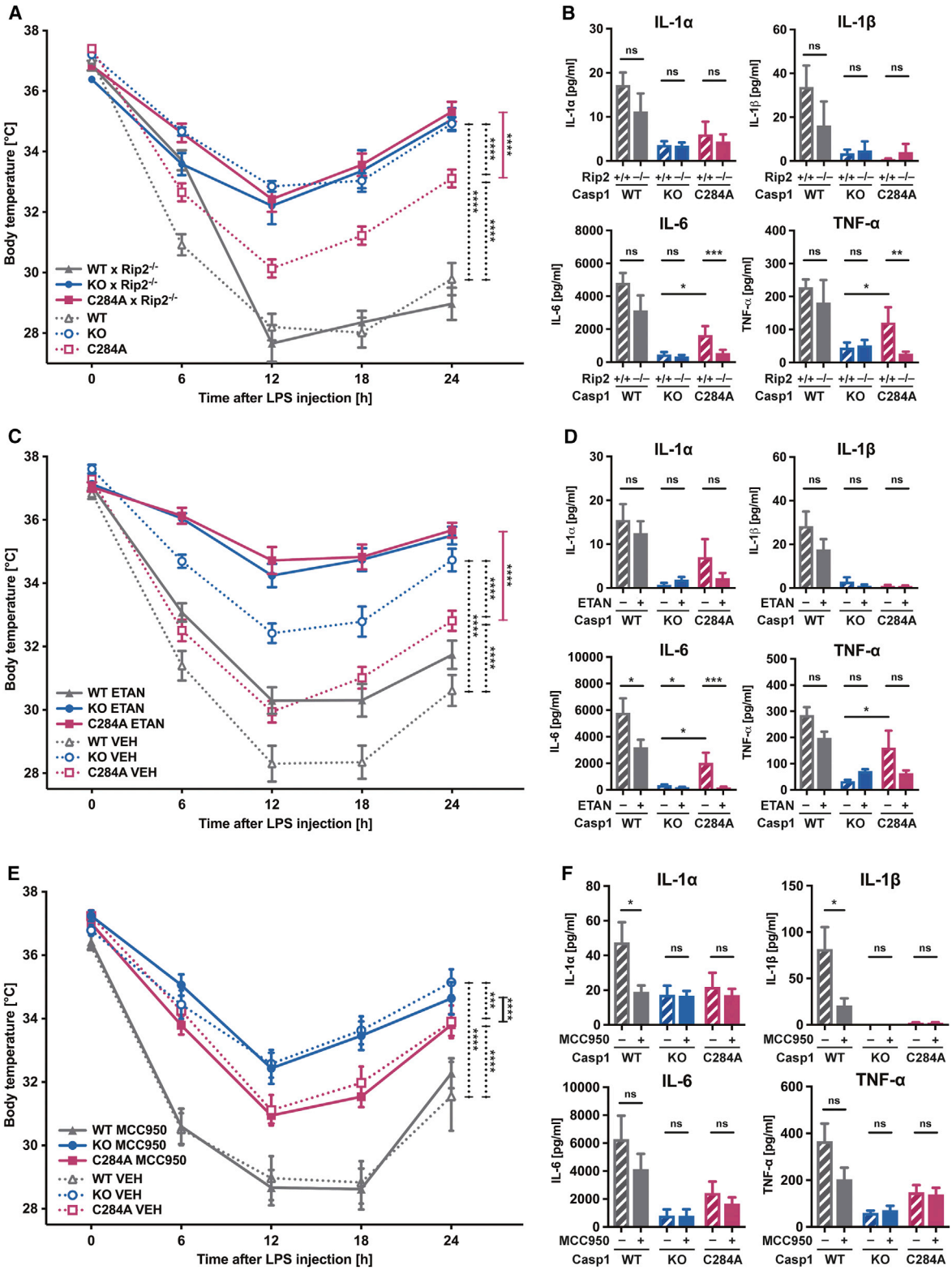

Figure 2. Caspase-1-C284A Initiated Inflammation Is Rip2 Dependent and TNF-α Mediated

(A) Mice of the indicated genotypes were challenged with 10 mg/kg LPS i.p., and body temperature was measured every 6 h.

(B) Serum levels of indicated cytokines 24 h after LPS challenge. In (A) and (B), data are presented as mean ± SEM, n = 14–32 per group.

(legend continued on next page)

R26-C284A mice to a *Rip2*$^{-/-}$ background. R26-C284A/*Rip2*$^{-/-}$ mice phenocopied *Casp1*$^{-/-}$ mice as they developed an equivalent hypothermia, while *Rip2* deficiency did not protect *Casp1*$^{+/+}$ or *Casp1*$^{-/-}$ mice from hypothermia (Figure 2A). Cytokine analysis revealed significantly reduced serum levels of IL-6 and TNF-α in R26-C284A/*Rip2*$^{-/-}$ mice compared with R26-C284A animals (Figure 2B). In contrast, *Casp1*$^{+/+}$ and *Casp1*$^{+/+}$/*Rip2*$^{-/-}$ as well as *Casp1*$^{-/-}$ and *Casp1*$^{-/-}$/*Rip2*$^{-/-}$ mice showed comparable inflammatory responses to LPS with respect to hypothermia or IL-6 and TNF-α secretion (Figures 2A and 2B). This indicates that caspase-1-C284A-mediated pro-inflammatory signaling is RIP2 dependent *in vivo*.

Because IL-6 acts downstream of TNF-α and is considered more a marker of inflammation than a key player in inflammasome mouse models, we blocked TNF-α signaling using etanercept in order to analyze its role in caspase-1-C284A-mediated signaling (McGeough et al., 2012; Peppel et al., 1991). Similar to *Rip2* deficiency, TNF-α blockade substantially reduced LPS induced inflammation in R26-C284A mice and mitigated hypothermia to the level of *Casp1*$^{-/-}$ mice (Figure 2C). Although etanercept protected *Casp1*$^{+/+}$ and *Casp1*$^{-/-}$ mice from hypothermia to some extent, enzymatically active caspase-1 in WT mice was able to promote severe inflammation upon LPS application despite of TNF-α blockade (Figure 2C). Etanercept reduced IL-6 and TNF-α secretion in R26-C284A mice to the level of *Casp1*$^{-/-}$ mice (Figure 2D). Although etanercept induced a statistically significant reduction of IL-6 secretion in *Casp1*$^{+/+}$ and *Casp1*$^{-/-}$ mice, the relative reduction in IL-6 secretion was much stronger for R26-C284A mice (1.8-fold for *Casp1*$^{+/+}$ and *Casp1*$^{-/-}$ versus 11.7-fold for R26-C284A). Hence, pro-inflammatory signaling induced by enzymatically inactive caspase-1 is mediated by TNF-α. In WT mice, etanercept failed to reduce IL-6 levels to values displayed by *Casp1*$^{-/-}$ mice, probably because of caspase-1 activity and subsequent IL-1β/NF-κB mediated induction of IL-6 gene expression.

When used *in vivo*, LPS stimulation induces TLR signaling and NLRP3 inflammasome activation. Hence, we tested whether NLRP3 activity is required for induction of pro-inflammatory signaling mediated by enzymatically inactive caspase-1. We used the NLRP3-specific inhibitor MCC950 prior to LPS application *in vivo* (Coll et al., 2015). As expected, chemical inhibition of the NLRP3 inflammasome led to strong reduction of IL-1β levels in serum of WT mice compared with controls and thereby proved that NLRP3 inhibition had been effective (Figure 2F). Surprisingly, the NLRP3 inhibition and resulting IL-1β reduction did not affect hypothermia in WT mice. Furthermore, NLRP3 inhibition failed to attenuate the hypothermia of R26-C284A or *Casp1*$^{-/-}$ mice, thereby not affecting caspase-1-C284A-mediated signaling (Figure 2E). In accordance with the unchanged temperature levels, IL-6 and TNF-α levels in the serum of R26-C284A mice were still elevated compared with *Casp1*$^{-/-}$ mice despite NLRP3 inhibition.

Taken together, our data demonstrate a non-enzymatic function of caspase-1 that induces RIP2-dependent, TNF-α-mediated inflammation *in vivo*. This caspase-1 pathway can be clearly separated from classical caspase-1 signaling depending on its enzymatic activity. Hence, we suggest to refer to this pathway as "non-canonical caspase-1 signaling."

Heterozygous Expression of Enzymatically Inactive Caspase-1 from Its Endogenous Locus Resembles the Human Genotype

To exclude potential locus and promoter dependent side effects in R26-C284A mice, we generated a second genomic mouse model using CRISPR/Cas9 technology and introduced the inactivating mutation p.C284A into the endogenous murine *Casp1* genomic locus (Figures S3A and S3B). Expression analysis revealed comparable RNA and protein levels between WT pro-caspase-1 and pro-caspase-1$^{C284A/C284A}$ mice in various tissues (Figures S3C and S3D). Identical to R26-C284A mice, *Casp1*$^{C284A/C284A}$ mice developed normally (Figures S3F–S3H) and did not show any obvious symptoms of spontaneous autoinflammation under SPF husbandry.

In order to analyze *Casp1*$^{C284A/C284A}$ mice *in vivo*, we challenged these animals by i.p. injection of LPS. Similar to R26-C284A mice, *Casp1*$^{C284A/C284A}$ mice developed increased hypothermia compared with *Casp1*$^{-/-}$ mice, thereby indicating a more severe inflammatory reaction mediated by enzymatically inactive caspase-1 (Figure 3A). Again, WT mice showed a stronger hypothermia than *Casp1*$^{C284A/C284A}$ mice (Figure 3A). Expression of mutant caspase-1-C284A from its endogenous locus allowed heterozygous expression of WT and mutant caspase-1 in Mendelian gene ratios and therefore resembles the genotype of the reported patients (Heymann et al., 2014; Luksch et al., 2013). Interestingly, these heterozygous mice (*Casp1*$^{WT/C284A}$) developed a similar degree of hypothermia as WT mice (Figure 3A). As expected, cytokine analysis revealed relevant levels of IL-1 only in mice expressing enzymatically active caspase-1. Furthermore, we found increased levels of IL-6 and TNF-α in serum of *Casp1*$^{C284A/C284A}$ mice compared with *Casp1*$^{-/-}$ mice (Figure 3B).

In order to prove the RIP2 dependency of caspase-1-C284A-mediated signaling in the second mouse model, we crossed *Casp1*$^{C284A/C284A}$ mice to a *Rip2*$^{-/-}$ background. Again, *Casp1*$^{C284A/C284A}$/*Rip2*$^{-/-}$ mice were protected from caspase-1-C284A-mediated inflammation and developed a hypothermia equivalent to *Casp1*$^{-/-}$ mice (Figure 3C). Cytokine analysis revealed significantly reduced serum levels of IL-6 and TNF-α in *Casp1*$^{C284A/C284A}$/*Rip2*$^{-/-}$ mice compared with *Casp1*$^{C284A/C284A}$ animals (Figure 3D). No differences between *Casp1*$^{+/+}$ and *Casp1*$^{+/+}$/*Rip2*$^{-/-}$ or *Casp1*$^{-/-}$ and *Casp1*$^{-/-}$/*Rip2*$^{-/-}$ mice were detected with respect to hypothermia or IL-6 and TNF-α secretion (Figures 3C and 3D).

Blocking of TNF-α signaling using etanercept reduced hypothermia and IL-6 levels of *Casp1*$^{C284A/C284A}$ mice to the level of *Casp1*$^{-/-}$ mice, thereby confirming the TNF-α dependency of *Casp1*$^{C284A/C284A}$-induced inflammation (Figures 3E and 3F).

(C and D) Etanercept (20 mg/kg intravenous [i.v.]) or vehicle was injected 1 h prior to LPS injection (10 mg/kg i.p.). Body temperature and cytokines were measured as described for (A) and (B). Data are presented as mean ± SEM, n = 17–32 per group.
(E and F) MCC950 (50 mg/kg i.v.) or vehicle was injected 2 h prior to LPS injection (10 mg/kg i.p.). Body temperature and cytokines were measured as described for (A) and (B). Data are presented as mean ± SEM, n = 13–24 per group.

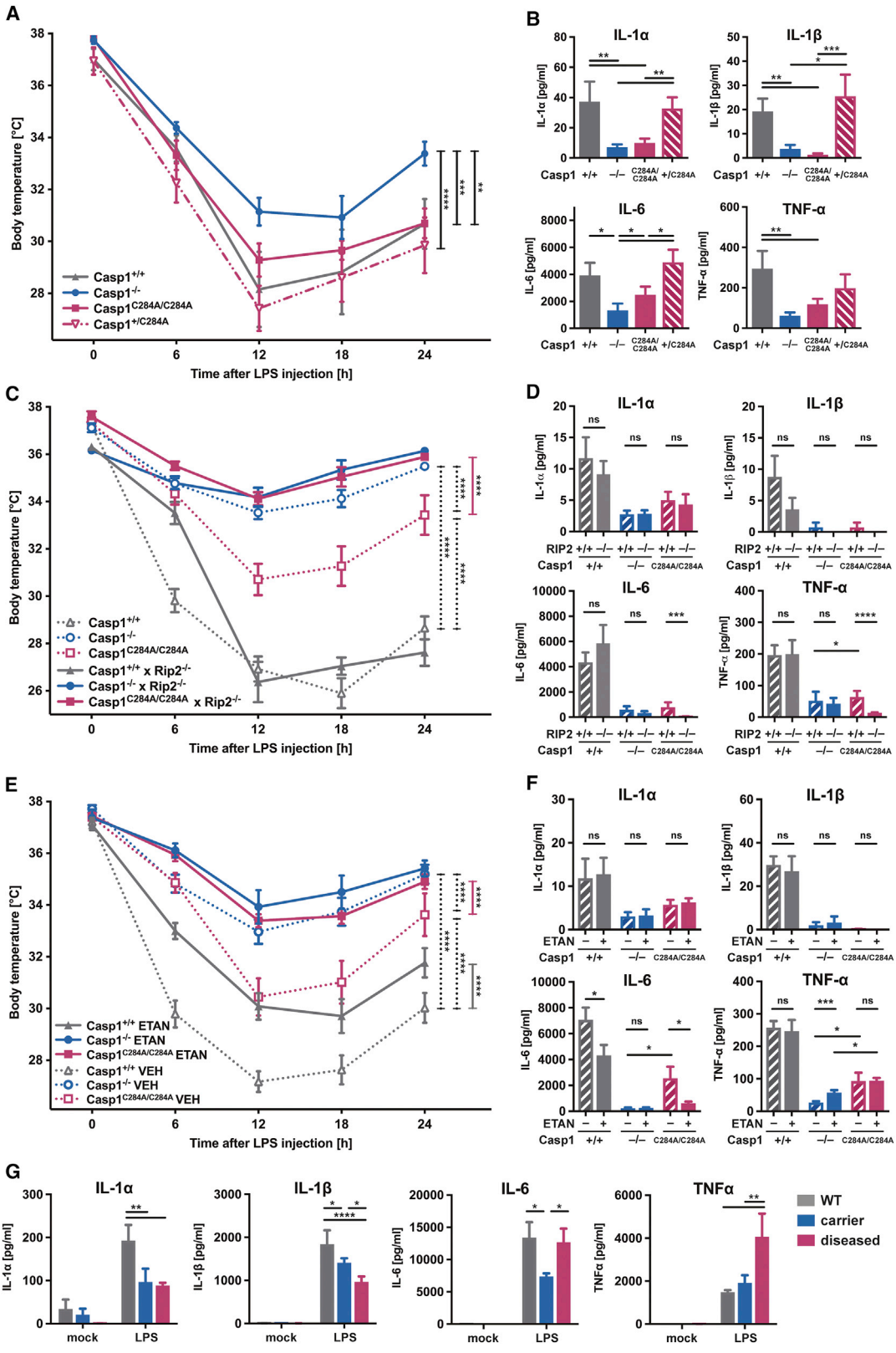

(legend on next page)

Likewise, IL-6 levels were reduced in etanercept treated WT mice, whereas TNF-α levels per se were not affected by the TNF-α blockade.

Human Caspase-1 Mutants with Reduced Enzymatic Activity Induce Enhanced TNF-α Secretion

To evaluate the role of TNF-α in humans carrying loss-of-function missense mutations in *CASP1*, we stimulated whole blood from healthy human donors and individuals with loss-of-function missense mutations with LPS. We divided carriers of *CASP1* missense mutations into two different groups on the basis of their clinical presentation. Individuals who had histories of unexplained recurrent autoinflammatory symptoms were assigned to the "diseased" group, while asymptomatic individuals were assigned to the "healthy carrier" group. At the time of the blood draw, all participating individuals were healthy, without any signs of autoinflammatory or infectious diseases. As expected, individuals carrying *CASP1* loss-of-function missense mutations revealed a reduced secretion of IL-1 cytokines, with the group of "diseased" patients featuring the strongest IL-1β reduction (Figure 3G). Interestingly, diseased but not healthy carriers of these mutations, showed enhanced TNF-α secretion compared with healthy controls. These differences in TNF-α expression may be explained by the inverse correlation between caspase-1 enzymatic activity and NF-κB activation as shown *in vitro* earlier (Heymann et al., 2014) and indicate the relevance of this non-canonical caspase-1 pathway in humans. However, IL-6 levels did not correlate with TNF-α secretion: healthy controls offered the same IL-6 levels as "diseased" patients, while healthy carriers revealed a reduction in IL-6 secretion.

Caspase-1-C284A Induces Severe Local Inflammation

Next, we analyzed the role of enzymatically inactive caspase-1 in a model of local inflammation. Therefore, we induced a local peritonitis by injecting a low LPS dose into the peritoneal cavity and subsequently analyzed the influx of neutrophils and monocytes as surrogates of local inflammation (Figures 4A and 4B). Following LPS injection, *Casp1*$^{C284A/C284A}$ mice showed the strongest influx of neutrophils and monocytes to the peritoneal cavity, thereby offering a more severe local inflammation compared with caspase-1 WT (Figure 4B). Interestingly, *Casp1*$^{-/-}$ mice showed slightly elevated numbers of infiltrating neutrophils and monocytes compared with WT mice. In this situation, peritoneal cells of *Casp1*$^{-/-}$ and *Casp1*$^{C284A/C284A}$ mice, both lacking enzymatic activity of caspase-1, offered reduced cell death compared with *Casp1*$^{+/+}$ mice (Figure 4C). Furthermore, LPS-stimulated splenocytes of *Casp1*$^{-/-}$ and R26-C284A mice did not cleave gasdermin D into its active fragment (Figure 4D). Hence, in this model of local peritonitis, enzymatically inactive caspase-1 drives inflammation independent of gasdermin D cleavage and cell death rates.

DISCUSSION

Here, we demonstrate that inactive caspase-1-C284A initiates pro-inflammatory, non-canonical caspase-1 signaling *in vivo*. Caspase-1-C284A-mediated signaling enhanced the expression of NF-κB-regulated cytokines such as IL-6 and TNF-α compared with *Casp1*$^{-/-}$ *in vivo*. The high levels of IL-6 and TNF-α found in *Casp1*$^{+/+}$ mice may be explained by activation of NF-κB downstream of TLRs and IL-1 receptors, activated by pyroptosis-related DAMP leakage and secreted IL-1 cytokines, both of which depend on the enzymatic activity of caspase-1. Therefore, our results do not allow us to determine if caspase-1 WT is also suited to induce non-canonical caspase-1 signaling *in vivo* or if this pathway is exclusively induced by enzymatically inactive caspase-1.

Overexpression of murine caspase-1 WT or C284A mutant in HEK293T cells confirmed the activation of NF-κB in contrast to control. In comparison with the *in vivo* experiments, overexpression of caspase-1 WT in HEK293T cells did not lead to enhanced activation compared with caspase-1-C284A. This finding is in line with previously published data (Heymann et al., 2014). As HEK293T cells express RIP2 protein, but lack the expression of *CASP1* and the inflammasome-associated genes *ASC*, *NLRP3*, *IL1A*, *IL1B*, and *IL18*, the activation of NF-κB through IL-1 cytokines and their receptors are missing in HEK293T cells (Thul et al., 2017). Furthermore, as protein-protein interactions between CASP1 and RIP2 are known to be enhanced for *CASP1* loss-of-function missense mutants, this mechanism may contribute to enhanced NF-κB activation induced by Casp1 C284A (Heymann et al., 2014).

The level of secreted IL-18 in *Casp1*$^{-/-}$ and R26-C284A mice was unexpected because of the abrogated enzymatic activity of caspase-1 in both mouse lines. However, caspase-1-independent activation of IL-18 by caspase-8 has been demonstrated in several studies (Bossaller et al., 2012; Formanowicz et al., 2018; Moriwaki et al., 2015; Pierini et al., 2013), and caspase-8 activation has been shown to occur mainly in the absence of caspase-1 enzymatic activity (Lee et al., 2018; Schneider et al., 2017; Van Opdenbosch et al., 2017). As Fas-ligand-induced

Figure 3. Heterozygous Expression of Enzymatically Inactive Caspase-1 from Its Endogenous Locus Resembles the Human Genotype

(A and B) Mice of the indicated genotypes were challenged with 10 mg/kg LPS i.p., and body temperature and cytokines were analyzed as described for Figures 1A and 1B. Data are presented as mean ± SEM, n = 9–14 per group.

(C and D) Mice of the indicated genotypes were challenged with 10 mg/kg LPS i.p., and body temperature and cytokines were analyzed as described for Figures 1A and 1B. Data are presented as mean ± SEM, n = 5–20 per group.

(E and F) Etanercept (20 mg/kg i.v.) or vehicle was injected 1 h prior to LPS injection (10 mg/kg i.p.). Body temperature and cytokines were measured as described for Figures 1A and 1B. Data are presented as mean ± SEM, n = 9–18 per group.

(G) Whole blood from healthy human donors (WT, n = 4) and patients with *CASP1* loss-of-function missense mutations either with (diseased, n = 6) or without (healthy carrier, n = 7) histories of recurrent autoinflammatory symptoms were stimulated with LPS and analyzed for indicated cytokines (genotypes of diseased patients: *CASP1*$^{R221C/WT}$, *CASP1*$^{K319R/R240Q}$, *CASP1*$^{R240Q/R240Q}$, *CASP1*$^{L265S/WT}$, *CASP1*$^{L265S/WT}$, and *CASP1*$^{A329T/WT}$; genotypes of healthy carriers: *CASP1*$^{R221C/WT}$, *CASP1*$^{R221C/WT}$, *CASP1*$^{R240Q/WT}$, *CASP1*$^{R240Q/WT}$, *CASP1*$^{R240Q/WT}$, *CASP1*$^{K319R/WT}$, and *CASP1*$^{A329T/WT}$). Data are presented as mean ± SEM.

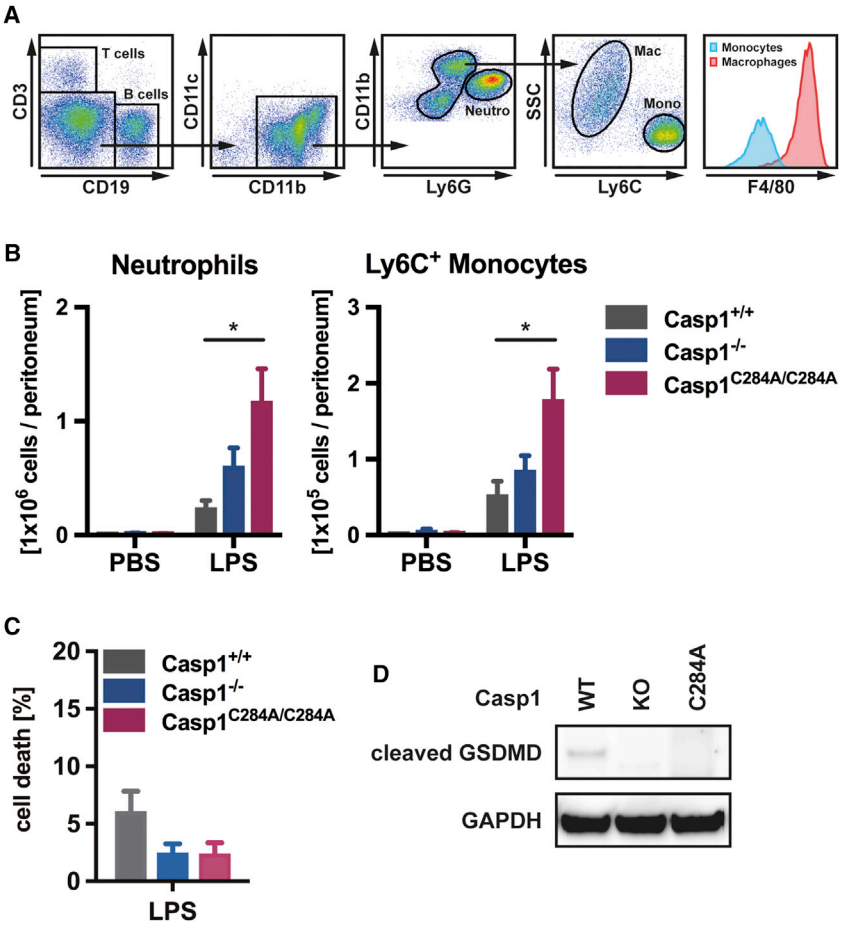

Figure 4. Caspase-1-C284A Induces Severe Local Inflammation

(A–C) Mice of the indicated genotypes were challenged with 50 ng LPS i.p., and influx of neutrophils and monocytes was analyzed using flow cytometry 6 h later. (A) Gating strategy: neutrophils ($CD3^-$, $CD19^-$, $CD11b^+$, $CD11c^{low}$, $Ly6G^{high}$), monocytes ($CD3^-$, $CD19^-$, $CD11b^+$, $CD11c^{low}$, $Ly6G^-$, $Ly6C^+$). (B) Data are presented as mean ± SEM, n = 6–8 per group. (C) Cell death of peritoneal cells following i.p. LPS was analyzed using flow cytometry. Data are presented as mean ± SEM, n = 6–8 per group. (D) Spleen lysates of *Casp1*$^{+/+}$, *Casp1*$^{-/-}$, and R26-C284A mice were analyzed for GSDMD cleavage 5 h after 10 mg/kg LPS *in vivo*.

caspase-8 activation is able to activate IL-18, and TNF-α is known to positively regulate activity of the Fas receptor, enhanced expression of TNF-α in R26-C284A mice may lead to enhanced processing and secretion of IL-18 (Bossaller et al., 2012; Elzey et al., 2001). Furthermore, signaling of TNF-α through TNFR1 receptor is also known to induce caspase-8 activation and may further contribute to enhanced caspase-8-mediated IL-18 processing in R26-C284A mice (Wang et al., 2008). Besides IL-18, active caspase-8 is also known to proteolytically cleave IL-1β (Bossaller et al., 2012; Maelfait et al., 2008; Moriwaki et al., 2015). Therefore, it is unclear why IL-1β secretion was not enhanced in R26-C284A mice. However, caspase-8-mediated IL-1β processing in bone marrow-derived dendritic cells (BMDCs) with absent enzymatic activity of caspase-1 leads to low IL-1β levels compared with caspase-1 WT mediated IL-1β processing *in vitro* (Schneider et al., 2017). Furthermore, the *in vivo* half-lives of IL-1β and IL-18 differ significantly (20 min versus 16 h) (Hosohara et al., 2002; Kudo et al., 1990). Therefore, detection of differential IL-1β secretion in R26-C284A versus *Casp1*$^{-/-}$ animals might be missed *in vivo*, while it could be detected for IL-18.

Caspase-1-C284A-expressing mice on *Rip2*$^{-/-}$ background were protected from hypothermia and IL-6/TNF-α secretion, thereby confirming the RIP2 dependency of non-canonical caspase-1 signaling. In contrast to previous studies, *Rip2* deficiency did not protect *Casp1*$^{+/+}$ or *Casp1*$^{-/-}$ mice from pro-inflammatory signaling (Chin et al., 2002; Nembrini et al., 2009). However, both studies used higher LPS dosing, thereby potentially inducing different effects.

Etanercept treatment attenuates hypothermia of R26-C284A or *Casp1*$^{C284A/C284A}$ mice to *Casp1*$^{-/-}$ levels, thereby proving the TNF-α dependency of caspase-1-C284A-mediated inflammation. Etanercept treatment of *Casp1*$^{+/+}$ animals also protects from hypothermia to some extent, as seen in other studies (McGeough et al., 2017; Nakayama et al., 2012), but not to the level observed in *Casp1*$^{-/-}$ mice. Hypothermia is a thermoregulatory response to systemic inflammation mediated by TNF-α, IL-1 cytokines, and leukotrienes (Bauss et al., 1987; Vanden Berghe et al., 2014; Leon, 2004; Paul et al., 1999; Singh et al., 2005). As WT mice, in contrast to *Casp1*$^{C284A/C284A}$ and *Casp1*$^{-/-}$ mice, offer enzymatic activity of caspase-1, this residual hypothermia is not a matter of etanercept efficiency but may be mediated by IL-1 cytokines processed by caspase-1 WT following LPS stimulation. Etanercept treatment led to unchanged or even enhanced levels of TNF-α in *Casp1*$^{+/+}$ or *Casp1*$^{-/-}$ mice despite protecting from hypothermia (Figures 2D and 3F). However, binding of etanercept to TNF-α is known to stabilize and enhance the total TNF-α mass *in vivo* (Kotyla et al., 2015; Mann et al., 2008), and ELISAs quantify total TNF-α and not the free biological active form. Therefore, etanercept may protect from hypothermia, despite unchanged or even increased TNF-α levels.

Inhibition of NLRP3 using MCC950 did not change hypothermia or IL-6/TNF-α levels. As chemical inhibitors may not be able to achieve full inhibition of their targets, it remains unclear if low residual NLRP3 activity is required and sufficient to induce caspase-1-C284A-mediated signaling or if this pathway is completely independent from the NLRP3 inflammasome. Interestingly, MCC950 led to reduction of IL-1α levels in *Casp1*$^{+/+}$ mice. However, these results are in line with our finding that following i.p. LPS, *Casp1*$^{-/-}$ mice offer lower IL-1α levels

compared with WT controls (see Figures 1B and 3B). In contrast to the current assumption from the literature that IL-1α secretion is dependent solely on caspase-11 following LPS stimulation *in vivo* (Kayagaki et al., 2011), our data suggest an additional role for NLRP3-dependent activation of caspase-1. However, compared with the published data (Kayagaki et al., 2011), we analyzed cytokine levels *in vivo* at a later time point at which DAMP-induced canonical NLRP3/caspase-1 activation may contribute to IL-1α secretion.

The human whole-blood assays showed reduced secretion of IL-1 cytokines for individuals carrying *CASP1* loss-of-function missense mutations whereby "diseased" patients within this group featured the strongest IL-1β reduction. The difference between these groups is in line with published *in vitro* data, as caspase-1 genotypes in the group of diseased patients were known to offer lower enzymatic activity than those found in the group of healthy carriers (Luksch et al., 2013). In autosomal-dominant inherited diseases with reduced penetrance, healthy carriers of disease-related mutations can be found within affected families. Additional genetic, environmental, and lifestyle factors contribute to the clinical onset of the respective disease. Although it is actually not clear if *CASP1* missense mutations lead to a clear-cut monogenetic disease, variable penetrance may explain the fact that some genotypes occur in the group of "diseased" and "healthy carriers" as well. The high TNF-α secretion of diseased patients indicates the relevance of non-canonical caspase-1 signaling in humans. In contrast to the mouse models, TNF-α levels in human healthy controls are low compared with diseased patients, and IL-6 levels do not correlate with TNF-α. However, mouse models built in order to mimic the human situation often offer differences when analyzed in detail while representing the human situation in a more general view (Brydges et al., 2009; Chae et al., 2011).

Non-canonical caspase-1 signaling does not necessarily lead to enhanced inflammation compared with inflammasome-activated signaling of caspase-1 WT but clearly induces different downstream mediators. However, caspase-1-C284A did enhance inflammation compared with WT in a model of local peritonitis. In this scenario, increased numbers of peritoneal neutrophils in absence of caspase-1 activity might also result from reduced pyroptosis due to impaired GSDMD cleavage, which is known to enhance inflammation under certain circumstances (Kambara et al., 2018). However, this mechanism cannot contribute to enhanced peritonitis of $Casp1^{C284A/C284A}$ mice compared with $Casp1^{-/-}$ mice, as both strains lack caspase-1 activity. Comparing the models of local and systemic inflammation used in this study indicates that the strength of the pro-inflammatory signal provided by caspase-1-C284A may depend on the type of inflammatory model used.

Taken together, we demonstrate that inactive caspase-1-C284A initiates pro-inflammatory, non-canonical caspase-1 signaling *in vivo*. This pathway depends on RIP2 and TNF-α but seems to be independent of NLRP3 activity. In contrast to WT animals suffering from caspase-1/IL-1-driven inflammation, mice carrying two alleles of enzymatically inactive caspase-1 suffer from TNF-α-driven inflammation induced by non-canonical caspase-1 signaling. As all known human patients with loss-of-function mutations in *CASP1* possess at least residual caspase-1 activity, they might benefit from dual anti-IL-1 and anti-TNF-α directed therapy.

STAR★METHODS

Detailed methods are provided in the online version of this paper and include the following:

- KEY RESOURCES TABLE
- LEAD CONTACT AND MATERIALS AVAILABILITY
- EXPERIMENTAL MODEL AND SUBJECT DETAILS
  - Mice
  - Murine BM-derived cells
  - Human cell lines
  - Human whole blood
- METHOD DETAILS
  - *In vivo* LPS application
  - Peritonitis model
  - Cytokine analysis
  - Flow cytometry
  - Histopathology
  - Plasmids
  - Transient transfection
  - NFκB luciferase reporter assay
  - Whole blood assay
  - Gene expression analysis
  - Western blot
- QUANTIFICATION AND STATISTICAL ANALYSIS
- DATA AND CODE AVAILABILITY

SUPPLEMENTAL INFORMATION

Supplemental Information can be found online at https://doi.org/10.1016/j.celrep.2020.01.090.

ACKNOWLEDGMENTS

We thank Kathrin Höhne, Christa Haase, Tobias Häring, and Christina Hiller for excellent technical assistance. We also thank Thomas Wunderlich (University of Cologne, Germany) for providing the *Rosa26* targeting vector. The study was supported by the German Research Foundation (DFG grants KFO249, TP1, WI 4269/1-2, and TP2, HO 4510/1-2) and the German Federal Ministry of Education and Research (PID-NET, Project A4). Open Access was supported by the Publication Fund of the TU Dresden, Germany.

AUTHOR CONTRIBUTIONS

S.R., A.R.-W., J.R., F.P., and S.W. conceptualized the project. S.R., M.L., H.L., A.G., and S.R.H. performed experiments. H.H.D. performed the statistical analysis. S.G. performed the histological analysis. R.B. and A.R. provided the targeting vector and expertise. R.N. and M.S. generated the transgenic mice. A.A.B.R. and M.A.C. provided inhibitors and expertise. S.R. and S.W. analyzed the data and wrote the manuscript. J.R., A.R.-W., and F.P. edited the manuscript.

DECLARATION OF INTERESTS

The authors declare no competing interests.

Received: April 30, 2019
Revised: December 10, 2019
Accepted: January 24, 2020
Published: February 25, 2020

REFERENCES

Bauss, F., Dröge, W., and Männel, D.N. (1987). Tumor necrosis factor mediates endotoxic effects in mice. Infect. Immun. *55*, 1622–1625.

Bossaller, L., Chiang, P.I., Schmidt-Lauber, C., Ganesan, S., Kaiser, W.J., Rathinam, V.A.K., Mocarski, E.S., Subramanian, D., Green, D.R., Silverman, N., et al. (2012). Cutting edge: FAS (CD95) mediates noncanonical IL-1β and IL-18 maturation via caspase-8 in an RIP3-independent manner. J. Immunol. *189*, 5508–5512.

Brydges, S.D., Mueller, J.L., McGeough, M.D., Pena, C.A., Misaghi, A., Gandhi, C., Putnam, C.D., Boyle, D.L., Firestein, G.S., Horner, A.A., et al. (2009). Inflammasome-mediated disease animal models reveal roles for innate but not adaptive immunity. Immunity *30*, 875–887.

Case, C.L., Kohler, L.J., Lima, J.B., Strowig, T., de Zoete, M.R., Flavell, R.A., Zamboni, D.S., and Roy, C.R. (2013). Caspase-11 stimulates rapid flagellin-independent pyroptosis in response to Legionella pneumophila. Proc. Natl. Acad. Sci. U S A *110*, 1851–1856.

Chae, J.J., Cho, Y.H., Lee, G.S., Cheng, J., Liu, P.P., Feigenbaum, L., Katz, S.I., and Kastner, D.L. (2011). Gain-of-function Pyrin mutations induce NLRP3 protein-independent interleukin-1β activation and severe autoinflammation in mice. Immunity *34*, 755–768.

Chin, A.I., Dempsey, P.W., Bruhn, K., Miller, J.F., Xu, Y., and Cheng, G. (2002). Involvement of receptor-interacting protein 2 in innate and adaptive immune responses. Nature *416*, 190–194.

Coll, R.C., Robertson, A.A.B., Chae, J.J., Higgins, S.C., Muñoz-Planillo, R., Inserra, M.C., Vetter, I., Dungan, L.S., Monks, B.G., Stutz, A., et al. (2015). A small-molecule inhibitor of the NLRP3 inflammasome for the treatment of inflammatory diseases. Nat. Med. *21*, 248–255.

Elzey, B.D., Griffith, T.S., Herndon, J.M., Barreiro, R., Tschopp, J., and Ferguson, T.A. (2001). Regulation of Fas ligand-induced apoptosis by TNF. J. Immunol. *167*, 3049–3056.

Formanowicz, D., Gutowska, K., and Formanowicz, P. (2018). Theoretical studies on the engagement of interleukin 18 in the immuno-inflammatory processes underlying atherosclerosis. Int. J. Mol. Sci. *18*, E3476.

Fritsch, M., Günther, S.D., Schwarzer, R., Albert, M.C., Schorn, F., Werthenbach, J.P., Schiffmann, L.M., Stair, N., Stocks, H., Seeger, J.M., et al. (2019). Caspase-8 is the molecular switch for apoptosis, necroptosis and pyroptosis. Nature *575*, 683–687.

Gewies, A., Gorka, O., Bergmann, H., Pechloff, K., Petermann, F., Jeltsch, K.M., Rudelius, M., Kriegsmann, M., Weichert, W., Horsch, M., et al. (2014). Uncoupling Malt1 threshold function from paracaspase activity results in destructive autoimmune inflammation. Cell Rep. *9*, 1292–1305.

Gong, Q., Long, Z., Zhong, F.L., Teo, D.E.T., Jin, Y., Yin, Z., Boo, Z.Z., Zhang, Y., Zhang, J., Yang, R., et al. (2018). Structural basis of RIP2 activation and signaling. Nat. Commun. *9*, 4993.

Heymann, M.C., Winkler, S., Luksch, H., Flecks, S., Franke, M., Ruß, S., Ozen, S., Yilmaz, E., Klein, C., Kallinich, T., et al. (2014). Human procaspase-1 variants with decreased enzymatic activity are associated with febrile episodes and may contribute to inflammation via RIP2 and NF-κB signaling. J. Immunol. *192*, 4379–4385.

Hosohara, K., Ueda, H., Kashiwamura, S., Yano, T., Ogura, T., Marukawa, S., and Okamura, H. (2002). Interleukin-18 induces acute biphasic reduction in the levels of circulating leukocytes in mice. Clin. Diagn. Lab. Immunol. *9*, 777–783.

Hoyos, B., Ballard, D.W., Böhnlein, E., Siekevitz, M., and Greene, W.C. (1989). Kappa B-specific DNA binding proteins: role in the regulation of human interleukin-2 gene expression. Science *244*, 457–460.

Kambara, H., Liu, F., Zhang, X., Liu, P., Bajrami, B., Teng, Y., Zhao, L., Zhou, S., Yu, H., Zhou, W., et al. (2018). Gasdermin D Exerts Anti-inflammatory Effects by Promoting Neutrophil Death. Cell Rep. *22*, 2924–2936.

Kang, S., Fernandes-Alnemri, T., Rogers, C., Mayes, L., Wang, Y., Dillon, C., Roback, L., Kaiser, W., Oberst, A., Sagara, J., et al. (2015). Caspase-8 scaffolding function and MLKL regulate NLRP3 inflammasome activation downstream of TLR3. Nat. Commun. *6*, 7515.

Kayagaki, N., Warming, S., Lamkanfi, M., Vande Walle, L., Louie, S., Dong, J., Newton, K., Qu, Y., Liu, J., Heldens, S., et al. (2011). Non-canonical inflammasome activation targets caspase-11. Nature *479*, 117–121.

Kotyla, P., Jankiewicz-Ziobro, K., Owczarek, A., and Kucharz, E.J. (2015). Etanercept increases tumor necrosis factor-alpha level but not sFas level in patients with rheumatoid arthritis. Isr. Med. Assoc. J. *17*, 14–18.

Kudo, S., Mizuno, K., Hirai, Y., and Shimizu, T. (1990). Clearance and tissue distribution of recombinant human interleukin 1 beta in rats. Cancer Res. *50*, 5751–5755.

Lallemand, Y., Luria, V., Haffner-Krausz, R., and Lonai, P. (1998). Maternally expressed PGK-Cre transgene as a tool for early and uniform activation of the Cre site-specific recombinase. Transgenic Res. *7*, 105–112.

Lamkanfi, M., Kalai, M., Saelens, X., Declercq, W., and Vandenabeele, P. (2004). Caspase-1 activates nuclear factor of the kappa-enhancer in B cells independently of its enzymatic activity. J. Biol. Chem. *279*, 24785–24793.

Lee, B.L., Mirrashidi, K.M., Stowe, I.B., Kummerfeld, S.K., Watanabe, C., Haley, B., Cuellar, T.L., Reichelt, M., and Kayagaki, N. (2018). ASC- and caspase-8-dependent apoptotic pathway diverges from the NLRC4 inflammasome in macrophages. Sci. Rep. *8*, 3788.

Leon, L.R. (2004). Hypothermia in systemic inflammation: role of cytokines. Front. Biosci. *9*, 1877–1888.

Liu, J., Guan, X., and Ma, X. (2007). Regulation of IL-27 p28 gene expression in macrophages through MyD88- and interferon-gamma-mediated pathways. J. Exp. Med. *204*, 141–152.

Luksch, H., Uckermann, O., Stepulak, A., Hendruschk, S., Marzahn, J., Bastian, S., Staufner, C., Temme, A., and Ikonomidou, C. (2011). Silencing of selected glutamate receptor subunits modulates cancer growth. Anticancer Res. *31*, 3181–3192.

Luksch, H., Romanowski, M.J., Chara, O., Tüngler, V., Caffarena, E.R., Heymann, M.C., Lohse, P., Aksentijevich, I., Remmers, E.F., Flecks, S., et al. (2013). Naturally occurring genetic variants of human caspase-1 differ considerably in structure and the ability to activate interleukin-1β. Hum. Mutat. *34*, 122–131.

Maelfait, J., Vercammen, E., Janssens, S., Schotte, P., Haegman, M., Magez, S., and Beyaert, R. (2008). Stimulation of Toll-like receptor 3 and 4 induces interleukin-1beta maturation by caspase-8. J. Exp. Med. *205*, 1967–1973.

Mann, D.L., Bozkurt, B., Torre-Amione, G., Soran, O.Z., and Sivasubramanian, N. (2008). Effect of the soluble TNF-antagonist etanercept on tumor necrosis factor bioactivity and stability. Clin. Transl. Sci. *1*, 142–145.

McGeough, M.D., Pena, C.A., Mueller, J.L., Pociask, D.A., Broderick, L., Hoffman, H.M., and Brydges, S.D. (2012). Cutting edge: IL-6 is a marker of inflammation with no direct role in inflammasome-mediated mouse models. J. Immunol. *189*, 2707–2711.

McGeough, M.D., Wree, A., Inzaugarat, M.E., Haimovich, A., Johnson, C.D., Peña, C.A., Goldbach-Mansky, R., Broderick, L., Feldstein, A.E., and Hoffman, H.M. (2017). TNF regulates transcription of NLRP3 inflammasome components and inflammatory molecules in cryopyrinopathies. J. Clin. Invest. *127*, 4488–4497.

Moriwaki, K., Bertin, J., Gough, P.J., and Chan, F.K.M. (2015). A RIPK3-caspase 8 complex mediates atypical pro-IL-1β processing. J. Immunol. *194*, 1938–1944.

Nakayama, M., Niki, Y., Kawasaki, T., Takeda, Y., Horiuchi, K., Sasaki, A., Okada, Y., Umezawa, K., Ikegami, H., Toyama, Y., and Miyamoto, T. (2012). Enhanced susceptibility to lipopolysaccharide-induced arthritis and endotoxin shock in interleukin-32 alpha transgenic mice through induction of tumor necrosis factor alpha. Arthritis Res. Ther. *14*, R120.

Nembrini, C., Kisielow, J., Shamshiev, A.T., Tortola, L., Coyle, A.J., Kopf, M., and Marsland, B.J. (2009). The kinase activity of Rip2 determines its stability and consequently Nod1- and Nod2-mediated immune responses. J. Biol. Chem. *284*, 19183–19188.

Paul, L., Fraifeld, V., and Kaplanski, J. (1999). Evidence supporting involvement of leukotrienes in LPS-induced hypothermia in mice. Am. J. Physiol. *276*, R52–R58.

Pellegrini, E., Desfosses, A., Wallmann, A., Schulze, W.M., Rehbein, K., Mas, P., Signor, L., Gaudon, S., Zenkeviciute, G., Hons, M., et al. (2018). RIP2 filament formation is required for NOD2 dependent NF-κB signalling. Nat. Commun. *9*, 4043.

Peppel, K., Crawford, D., and Beutler, B. (1991). A tumor necrosis factor (TNF) receptor-IgG heavy chain chimeric protein as a bivalent antagonist of TNF activity. J. Exp. Med. *174*, 1483–1489.

Pierini, R., Perret, M., Djebali, S., Juruj, C., Michallet, M.C., Förster, I., Marvel, J., Walzer, T., and Henry, T. (2013). ASC controls IFN-γ levels in an IL-18-dependent manner in caspase-1-deficient mice infected with Francisella novicida. J. Immunol. *191*, 3847–3857.

Ritz, C., Baty, F., Streibig, J.C., and Gerhard, D. (2015). Dose-Response Analysis Using R. PLoS ONE *10*, e0146021.

Rudaya, A.Y., Steiner, A.A., Robbins, J.R., Dragic, A.S., and Romanovsky, A.A. (2005). Thermoregulatory responses to lipopolysaccharide in the mouse: dependence on the dose and ambient temperature. Am. J. Physiol. Regul. Integr. Comp. Physiol. *289*, R1244–R1252.

Ruefli-Brasse, A.A., Lee, W.P., Hurst, S., and Dixit, V.M. (2004). Rip2 participates in Bcl10 signaling and T-cell receptor-mediated NF-kappaB activation. J. Biol. Chem. *279*, 1570–1574.

Saavedra, P.H.V., Demon, D., Van Gorp, H., and Lamkanfi, M. (2015). Protective and detrimental roles of inflammasomes in disease. Semin. Immunopathol. *37*, 313–322.

Sarkar, A., Duncan, M., Hart, J., Hertlein, E., Guttridge, D.C., and Wewers, M.D. (2006). ASC directs NF-kappaB activation by regulating receptor interacting protein-2 (RIP2) caspase-1 interactions. J. Immunol. *176*, 4979–4986.

Schneider, C.A., Rasband, W.S., and Eliceiri, K.W. (2012). NIH Image to ImageJ: 25 years of image analysis. Nat. Methods *9*, 671–675.

Schneider, K.S., Groß, C.J., Dreier, R.F., Saller, B.S., Mishra, R., Gorka, O., Heilig, R., Meunier, E., Dick, M.S., Ćiković, T., et al. (2017). The inflammasome drives GSDMD-independent secondary pyroptosis and IL-1 release in the absence of caspase-1 protease activity. Cell Rep. *21*, 3846–3859.

Serfling, E., Barthelmäs, R., Pfeuffer, I., Schenk, B., Zarius, S., Swoboda, R., Mercurio, F., and Karin, M. (1989). Ubiquitous and lymphocyte-specific factors are involved in the induction of the mouse interleukin 2 gene in T lymphocytes. EMBO J. *8*, 465–473.

Sica, A., Dorman, L., Viggiano, V., Cippitelli, M., Ghosh, P., Rice, N., and Young, H.A. (1997). Interaction of NF-kappaB and NFAT with the interferon-gamma promoter. J. Biol. Chem. *272*, 30412–30420.

Singh, V.P., Patil, C.S., Kumar, M., and Kulkarni, S.K. (2005). Effect of 5-lipoxygenase inhibitor against lipopolysaccharide-induced hypothermia in mice. Indian J. Exp. Biol. *43*, 1150–1155.

Stein, R., Kapplusch, F., Heymann, M.C., Russ, S., Staroske, W., Hedrich, C.M., Rösen-Wolff, A., and Hofmann, S.R. (2016). Enzymatically inactive procaspase 1 stabilizes the ASC pyroptosome and supports pyroptosome spreading during cell division. J. Biol. Chem. *291*, 18419–18429.

Thul, P.J., Åkesson, L., Wiking, M., Mahdessian, D., Geladaki, A., Ait Blal, H., Alm, T., Asplund, A., Björk, L., Breckels, L.M., et al. (2017). A subcellular map of the human proteome. Science *356*, eaal3321.

Van Opdenbosch, N., Van Gorp, H., Verdonckt, M., Saavedra, P.H.V., de Vasconcelos, N.M., Gonçalves, A., Vande Walle, L., Demon, D., Matusiak, M., Van Hauwermeiren, F., et al. (2017). Caspase-1 engagement and TLR-induced c-FLIP expression suppress ASC/caspase-8-dependent apoptosis by inflammasome sensors NLRP1b and NLRC4. Cell Rep. *21*, 3427–3444.

Vanden Berghe, T., Demon, D., Bogaert, P., Vandendriessche, B., Goethals, A., Depuydt, B., Vuylsteke, M., Roelandt, R., Van Wonterghem, E., Vandenbroecke, J., et al. (2014). Simultaneous targeting of IL-1 and IL-18 is required for protection against inflammatory and septic shock. Am. J. Respir. Crit. Care Med. *189*, 282–291.

Wang, L., Du, F., and Wang, X. (2008). TNF-alpha induces two distinct caspase-8 activation pathways. Cell *133*, 693–703.

Winkler, S., and Rösen-Wolff, A. (2015). Caspase-1: an integral regulator of innate immunity. Semin. Immunopathol. *37*, 419–427.

Zhu, Y.X., Kang, L.Y., Luo, W., Li, C.C., Yang, L., and Yang, Y.C. (1996). Multiple transcription factors are required for activation of human interleukin 9 gene in T cells. J. Biol. Chem. *271*, 15815–15822.

STAR★METHODS

KEY RESOURCES TABLE

REAGENT or RESOURCE	SOURCE	IDENTIFIER
Antibodies		
anti-Caspase-1 (p20, Casper-1)	AdipoGen	Cat# AG-20B-0042; RRID: AB_2490248
anti-β-Actin	Sigma-Aldrich	Cat# A5316; RRID: AB_476743
anti-Glyceraldehyde-3-Phosphate Dehydrogenase (GAPDH)	Meridian Life Science	Cat# H86045M; RRID: AB_497737
anti-mouse immunoglobulins/HRP	Dako	Cat# P0260; RRID: AB_2636929
FITC anti-mouse CD3 (clone 17A2)	BioLegend	Cat# 100203; RRID: AB_312660
PE anti-mouse CD3ε (clone 145-2C11)	BioLegend	Cat# 100307; RRID: AB_312672
Brilliant Violet 421 anti-mouse CD19 (clone 6D5)	BioLegend	Cat# 115549; RRID: AB_2563066
APC anti-mouse CD19 (clone 6D5)	BioLegend	Cat# 115511; RRID: AB_313646
FITC anti-mouse Ly-6C (clone HK1.4)	BioLegend	Cat# 128005; RRID: AB_1186134
PerCP/Cy5.5 anti-mouse CD11b (clone M1/70)	BioLegend	Cat# 101227; RRID: AB_893233
PE/Cy7 anti-mouse CD11c (clone N418)	BioLegend	Cat# 117317; RRID: AB_493569
Brilliant Violet 421 anti-mouse F4/ 80 (clone BM8)	BioLegend	Cat# 123137; RRID: AB_2563102
Brilliant Violet 510 anti-mouse Ly-6G (clone 1A8)	BioLegend	Cat# 127633; RRID: AB_2562937
PE/Cy7 anti-mouse CD8a (clone 53-6.7)	BioLegend	Cat# 100721; RRID: AB_312760
Brilliant Violet 510 anti-mouse CD4 (clone RM4-5)	BioLegend	Cat# 100559; RRID: AB_2562608
anti-mouse CD16/32	BioLegend	Cat# 101319; RRID: AB_1574973
Chemicals, Peptides, and Recombinant Proteins		
mGM-CSF	Immunotools	Cat# 12343123
Ultrapure LPS	InvivoGen	Cat# tlrl-3pelps
Standard LPS	InvivoGen	Cat# tlrl-eblps
Etanercept	Pfizer Pharma	CAS 185243-69-0
MCC950	(Coll et al., 2015)	CAS 210826-40-7
Collagenase D	Sigma Aldrich	Cat# 11088858001
DNase I	Sigma Aldrich	Cat# 10104159001
Zombie NIR Fixable Viability Dye	BioLegend	Cat# 423105
Polyethylenimine	Sigma Aldrich	Cat# 408727
Critical Commercial Assays		
Cytometric Bead Array - mouse (CBA)	BD	Cat# 558267
CBA mouse TNF Flex Set	BD	Cat# 558299
CBA mouse IL-6 Flex Set	BD	Cat# 558301
CBA mouse IL-1α Flex Set	BD	Cat# 560157
CBA mouse IL-1β Flex Set	BD	Cat# 560232
Cytometric Bead Array - human (CBA)	BD	Cat# 558264
CBA human TNF Flex Set	BD	Cat# 558273
CBA human IL-6 Flex Set	BD	Cat# 558276
CBA human IL-1α Flex Set	BD	Cat# 560153
CBA human IL-1β Flex Set	BD	Cat# 558279
Cytokine & Chemokine 26-Plex Mouse ProcartaPlex Panel 1	ThermoFisher	Cat# EPX260-26088-901
RNeasyMini Kit	QIAGEN	Cat# 74106
M-MLV Reverse Transcriptase	Promega	Cat# M1701
Random hexamers	Promega	Cat# C1181
Oligo(dT) primers	Promega	Cat# C1101

(*Continued on next page*)

Continued

REAGENT or RESOURCE	SOURCE	IDENTIFIER
Precision Count Beads	BioLegend	Cat# 424902
Dual-Luciferase Reporter Assay System	Promega	Cat# E1910
Experimental Models: Cell Lines		
Mouse: primary GM-CSF BM-derived cells	This manuscript	N/A
Human: HEK293T cells	ATCC	Cat# CRL-11268
Human: primary whole blood from patients and healthy volunteers	This manuscript	N/A
Experimental Models: Organisms/Strains		
Mouse: Rosa26$^{Casp1\text{-}C284A\text{-}Neo\text{-}Stop}$	This manuscript	N/A
Mouse: R26-C284A (R26$^{Casp1\text{-}C284A/Casp1\text{-}C284A}$/Casp1$^{-/-}$)	This manuscript	N/A
Mouse: Casp1$^{C284A/C284A}$	This manuscript	N/A
Mouse: Casp1$^{-/-}$	Yale University School of Medicine, New Haven	(Case et al., 2013)
Mouse: Rip2$^{-/-}$	Department of Immunology, Genentech, Inc.	(Ruefli-Brasse et al., 2004)
Mouse: R26-C284A/Rip2$^{-/-}$	This manuscript	N/A
Mouse: Casp1$^{-/-}$/Rip2$^{-/-}$	This manuscript	N/A
Mouse: Casp1$^{C284A/C284A}$/Rip2$^{-/-}$	This manuscript	N/A
Mouse: C57BL/6N	Charles River	C57BL/6NCrl
Oligonucleotides		
See Table S1		N/A
Recombinant DNA		
p.C284A Rosa26 targeting vector	This manuscript	N/A
p6NST53-Casp1-WT	This manuscript	N/A
p6NST53-Casp1-C284A	This manuscript	N/A
pBxIVluci	A gift from Prof. G. Nuñez, University of Michigan	N/A
pRL-TK	Promega	Cat# E2241
Software and Algorithms		
Prism 6	GraphPad	https://www.graphpad.com/scientific-software/prism/
ImageJ	https://imagej.nih.gov/ij/	(Schneider et al., 2012)
FCAP Array Software	BD	Cat# 652099
FlowJo 10	Treestar	https://www.flowjo.com/
R version 3.6.1	https://www.R-project.org/	The R Project for Statistical Computing
DRC package, version 3.0.1	https://cran.r-project.org/web/packages/drc/	(Ritz et al., 2015)

LEAD CONTACT AND MATERIALS AVAILABILITY

Further information and requests for reagents may be directed to and will be fulfilled by the Lead Contact Stefan Winkler (stefan.winkler@uniklinikum-dresden.de). All unique reagents and mouse lines generated in this study are available from the Lead Contact with a completed Materials Transfer Agreement.

EXPERIMENTAL MODEL AND SUBJECT DETAILS

Mice

Rosa26$^{Casp1\text{-}C284A}$ mice were generated using conditional gene targeting. In brief, the cDNA of c-terminally FLAG-tagged murine caspase-1 p.C284A was cloned into the *Rosa26* targeting vector pSerc, carrying a loxP-site flanked neomycin-Stop cassette between the CAG promotor and the cDNA. Following linearization with AsiSI, the construct was electroporated into Agouti C57BL/6N embryonic stem cells. PCR based screening for clones carrying the *Rosa26*$^{Casp1\text{-}C284A\text{-}Neo\text{-}Stop}$ allele (primer for 5′-TAGG TAGGGGATCGGGACTCT-3′; rev 5′-GCGAAGAGTTTGTCCTCAACC-3′) and analysis of correct integration of 5′- and 3′-arms using

Southern blotting (primer pairs for generation of radio labeled probes: 5′-arm: for 5′-GGAACCTCCTCCATCTGGATCCTCCCC-3′, rev 5′-CCTGCCTAGGGCGTGGAGAGCGATC-3′; 3′-arm: for 5′-GGTCCTGCTTGAACATTGCC-3′, rev 5′-GGACAAACACTTCTACATGT CAGTT-3′) revealed correct clones which were injected into C57BL/6NCRL morulae at the Transgenic Core Facility, MPI of Molecular Cell Biology and Genetics, Dresden (Figures S1A–S1C).

Casp1^{C284A} mice were generated using CRISPR/Cas9 with sgRNA 5′-ACCATCAGCACTTACCTCCA-3′ and repair oligo 5′-AA TCTTTCAGATGATGAACACTTTGAAGTGCCCAAGCTTGAAAGACAAGCCCAAGGTGATTATC ATCCAAGCTGCCAGAGGAGGTAA GTGCTGATGGTTTAAAATAACAGGGCATTCCCATTGAGACTTTATCATTTAT-3′ in C57BL/6NCRL mice purchased from Charles River (Sulzfeld, Germany) (Figure S2A).

Wild-type C57BL/6N mice were purchased from Charles River and bred in-house. *Casp1*$^{-/-}$ and *Rip2*$^{-/-}$ mice were described previously (Case et al., 2013; Ruefli-Brasse et al., 2004). All mice were housed at the Experimental Center, Technische Universität Dresden, Germany, under specific pathogen free conditions in individually ventilated cages. Male and female mice 9 to 14 weeks of age were used for all *in vivo* experiments and randomly assigned to experimental groups. All animal procedures were performed according to institutional guidelines and in accordance with the Landesdirektion Sachsen.

Murine BM-derived cells

Bone marrow was flushed from femurs of 8 – 14-week-old male and female mice of the indicated genotypes. GM-CSF differentiated, BM-derived cells were generated *in vitro* by culturing bone marrow cells in the presence of 20 ng/ml mGM-CSF for 6 days. Cells were plated 24 h before inflammasome stimulation. The cells were primed with ultrapure LPS 4 h (*E. coli* 0111:B4; InvivoGen) followed by activation of the NLRP3 inflammasome using 5 μM Nigericin for 30 min. GM-CSF differentiated, BM-derived cells were grown in Iscove's Basal Media (Merck Millipore) supplemented with 10% FCS (Merck Millipore), 100U/ml Penicillin (Invitrogen), 100U/ml Streptomycin (Invitrogen) and 2mM L-Glutamine (Invitrogen). Cells were grown at 37°C in a humidified atmosphere with 5% CO_2.

Human cell lines

HEK293T cells (ATCC) were grown in DMEM supplemented with 10% FCS (Merck Millipore), 100U/ml Penicillin (Invitrogen), 100U/ml Streptomycin (Invitrogen) and 2mM L-Glutamine (Invitrogen). Cells were grown at 37°C in a humidified atmosphere with 5% CO_2.

Human whole blood

Heparin coated tubes (Sarstedt 01.1604.001) were used to collect blood from male and female patients. The mean age was 21.5 years (range 4 - 46). The study was approved by the responsible ethics committee (Ethics committee of the TU Dresden, EK97032014) before start. Human whole blood was drawn after obtaining written informed consent.

METHOD DETAILS

In vivo LPS application

10 mg/kg LPS (*E.coli* 0111:B4, Invivogen) was injected intraperitoneally. Body temperature of mice was measured every 6 h for 24 h using a rodent rectal temperature probe. Blood samples for cytokine analysis of the serum were collected 24 h after injection by retroorbital blood draw or cardiac puncture of Ketamine/Xylazine anesthetized mice. Inhibitors were injected intravenously by retroorbital injection 1 h (Etanercept (20 mg/kg)) or 2 h (MCC950 (50 mg/kg)) prior to LPS injection. For all *in vivo* studies age and sex matched animals of the designated genotypes were used.

Peritonitis model

Peritonitis was induced by intraperitoneal injection of 50 ng LPS (*E.coli* 0111:B4, Invivogen) in a total volume of 400 μl PBS. 6 h after injection, mice were sacrificed and the peritoneum was flushed with 5 mL of PBS / 5 mM EDTA to harvest peritoneal cells. Subsequently, live cells were stained with surface antibodies and analyzed by flow cytometry. Precision Count Beads™ (BioLegend) were used to determine absolute peritoneal cell numbers.

Cytokine analysis

Serum IL-1α, IL-1β, IL-6 and TNF-α levels were measured by cytometric bead array (CBA, BD) according to the manufacturer's protocol using a BD LSR II flow cytometer. Results were analyzed with FCAP array software (BD). Cytokine multiplex analysis was performed using a Luminex® 200 platform using the Cytokine & Chemokine 26-Plex Mouse ProcartaPlex Panel 1 (Thermo Fisher Scientific) according to the manufacturer's protocol.

Flow cytometry

Single cell suspension from spleen tissues was prepared by physical disruption, followed by digestion with 1 mg/ml Collagenase D (Roche Diagnostics) and 0.1 mg/ml DNase I (Roche Diagnostics). Erythrocytes were lysed in RBC Lysis Buffer (BioLegend). Live/dead discrimination was performed by staining with Zombie NIR™ Fixable Viability Dye (BioLegend). Unspecific antibody binding was blocked with anti-mouse CD16/32 (TruStain fcX, clone 93, BioLegend). For surface staining, splenocytes or peritoneal cells were stained with FITC anti-mouse CD3 (17A2) or PE anti-mouse CD3ε (145-2C11), Brilliant Violet 421™ anti-mouse CD19 (6D5) or

APC anti-mouse CD19 (6D5), FITC anti-mouse Ly-6C (HK1.4), PerCP/ Cy5.5 anti-mouse CD11b (M1/70), PE/Cy7 anti-mouse CD11c (N418), Brilliant Violet 421™ anti-mouse F4/ 80 (BM8) and Brilliant Violet 510™ anti-mouse Ly-6G (1A8). Splenocytes were additionally incubated with PE/Cy7 anti-mouse CD8a (53-6.7) and Brilliant Violet 510™ CD4 (RM4-5). All surface antibodies were obtained from BioLegend. Stained cells were examined using a LSR II flow cytometer and data was analyzed using FlowJo software.

Histopathology

Organs were isolated from WT, *Casp1*$^{-/-}$ and *Rosa26*$^{Casp1\text{-}C284A}$ mice, fixed in 4% formalin, embedded in paraffin, sectioned, and stained with hematoxylin and eosin. Sections were then evaluated by a veterinary pathologist.

Plasmids

Plamids encoding murine wild-type and variant caspase-1 were generated as previously described (Stein et al., 2016). The cDNA of murine wild-type caspase-1 and C284A mutant were cloned into the vector p6NST53, thereby generating p6NST53-Casp1-WT and p6NST53-Casp1-C284A. All constructs underwent quality control by restriction enzyme digestion and Sanger sequencing. The p6NST53 vector was kindly provided by Prof. Dirk Lindemann (Institute of Virology, University Hospital Carl Gustav Carus, Technische Universität Dresden, Germany). The luciferase reporter plasmid pBxIVluci was a gift from Prof. G. Nuñez (University of Michigan, Ann Arbor, MI). The *Renilla* expressing plasmid pRL-TK (Promega) was used as a luciferase control reporter vector.

Transient transfection

HEK293T cells were seeded in 12-well plates. 24h later, cells were transfected with plasmids encoding murine wild-type or variant (C284A) caspase-1, the luciferase reporter plasmid pBxIVluci, the luciferase control reporter vector pRL-TK (Promega) or empty control vector using polyethylenimine. Samples were evaluated 24 h later using the Dual-Luciferase® Reporter Assay (Promega). For evaluation of cell death, transfected HEK293T cells were stained with Hoechst and propidium iodide (PI). For quantification of dead cells PI^+ cells were quantified using ImageJ software.

NFκB luciferase reporter assay

Following transient transfection of plasmids (see section "Transient transfection") NFκB activity was determined using the Dual-Luciferase® Reporter Assay System from Promega, according to the manufacturer's protocol. The activity of the luciferase was measured using a Mithras LB940 luminometer (Berthold).

Whole blood assay

Blood samples were distributed on 96-well plates using 140 μl per well, followed by stimulation using 1 μg/ml LPS for 6 h. Plates were incubated on a shaker (450 rpm) in a humidified incubator with 37°C, 5% CO_2. At the end of all stimulations 100 μL of PBS was added to each well, the plates were centrifuged (1200 rpm, 5 min, room temperature) and the supernatants were frozen at −80°C. IL-1α, IL-1β, IL-6 and TNF-α levels in the supernatant were analyzed using a cytometric bead assay (CBA, Becton Dickinson) according to the manufacturer's instructions.

Gene expression analysis

Total RNA from mouse tissues was purified using the RNeasy Mini kit (QIAGEN). Subsequently, first strand cDNA was generated using M-MLV Reverse Transcriptase (Promega) with random hexamer and oligo(dT) primers. Both kits were used according to the manufacturer's instructions. Gene expression analysis was performed as reported earlier (Luksch et al., 2011). The following primers were used: *Casp1* 5′- GGCCCCAGGCAAGCCAAATCT-3′ and 5′-CAGTCCTGGAAATGTGCCATC-3′, Rpl13A 5′- AGCCTAC CAGAAAGTTTGCTTAC-3′ and 5′-GCTTCTTCTTCCGATAGTGCATC-3′. All samples were run as triplicates and transcription levels were normalized to Rpl13A.

Western blot

Mouse organs were minced and incubated in RIPA buffer (50 mM Tris-HCl; 150 mM NaCl; 0.5% sodium deoxycholate; 1% Triton X-100) for cell lysis. KALB lysis buffer (50 mM Tris-HCl; 150 mM NaCl; 10 mM NaF; 1 mM EDTA; 1 mM Na_3VO_4; 1 mM PMSF; 1% Triton X-100; 2% protease inhibitor) was used for lysis of BMDCs. Passive lysis buffer (PLB, Promega) was used for cell lysis of HEK293T cells. Supernatant of BMDCs was precipitated by Methanol/Chloroform extraction. Protein samples were analyzed by SDS-PAGE and western blotting using anti-caspase-1 (p20) mouse (Casper-1, AdipoGen Life Science), anti-β-actin mouse antibody (Sigma-Aldrich) and anti-GAPDH (Meridian Life Science).

QUANTIFICATION AND STATISTICAL ANALYSIS

GraphPad Prism software was used to perform statistical analysis. Nonparametric Mann-Whitney test was used to compare cytokine levels, immune cell influx to the peritoneum or relative NFκB activation. Mean values (±SEM) are displayed in the figures and values of n are reported in the figure legends. 2-way ANOVA was used to analyze the human whole blood assay. P values ≤ 0.05 were defined as significant. Asterisks indicate significance levels (* $p \leq 0.05$, ** $p \leq 0.01$, *** $p \leq 0.001$ and **** $p \leq 0.0001$).

Using the software package "R," temperature time courses were compared pairwise using a nonlinear regression model. A physiologically motivated kinetic response model defined by the differential equation $dT(t)/dt = rT(t)(1-T(t)/C) - p_0 f(s,k)T(t)$ with $T(t = 0) = C$ was formulated and fitted to the time courses by means of a maximum likelihood procedure based on log-normally distributed temperature values. Thereby, T(t) is the predicted temperature at time point t and the kinetic parameters are: strength of temperature auto-regulation, r, normal body temperature, C, maximum damage, p_0, and clearance rate k. Function f(s,k) is the gamma density function with shape parameter s. The resulting curves stratified by genotype/inhibitor are pairwise compared on the basis of a likelihood-ratio-test. Of note, the estimated kinetic parameters are not relevant for our purpose of pairwise comparisons of the fitted curves.

DATA AND CODE AVAILABILITY

This study did not generate/analyze datasets/codes.